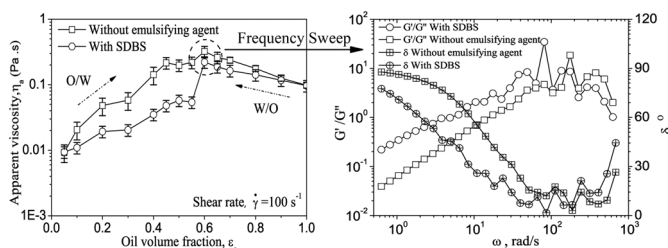


Apparent Viscosity of Oil-Water (Coarse) Emulsion and Its Rheological Characterization During the Phase Inversion Region

Jian Zhang, Jing-yu Xu, Meng-chen Gao, and Ying-xiang Wu

LMFS, Institute of Mechanics, Chinese Academy of Sciences, Beijing, P. R. China

GRAPHICAL ABSTRACT



A series of oil and water (coarse) emulsions has been systematically studied in order to obtain more knowledge about the flow characteristics. Experimental measurements were conducted using Rheo Stress 6000 from Therm O Haake. Several factors such as shear rate, oil volume fraction, temperature, emulsifying agent, and stirring time on the rheological characteristics of emulsions were investigated. The emulsions without emulsifying agent are discussed by Ostwald de Waele model, Casson model, and Bingham model, respectively, according to different oil volume fractions. Sixteen models of the apparent viscosity were evaluated to predict these emulsions. The results show that existing models of the apparent viscosity exhibit large deviations from the experimental data over the range of low and middle oil volume fractions ($\epsilon_o < 0.5$) due to the droplets fast flocculation, and but can give a good prediction at high oil volume fractions ($\epsilon_o > 0.6$). Furthermore, emulsifying agent and shear rate have few influences on the phase inversion point and the maximum value of the apparent viscosity appears around $\epsilon_o = 0.6$. At the phase inversion point, the viscoelastic behavior of the emulsions were also analyzed by shear stress sweeps and frequency sweeps, respectively. These findings are helpful to improve the pipeline transportation of an immiscible oil and water two-phase dispersed flow.

Keywords Apparent viscosity, emulsions, phase inversion region, rheology

1. INTRODUCTION

Oil and water two-phase emulsions may form during a diverse range of processes industries and particularly in the petroleum industry. Typically, the emulsions are

divided into two general categories: a dispersion of oil droplets in a continuous water phase (designated as oil-in-water, o/w) and a dispersion of water droplets in a continuous oil phase (designated as water-in-oil, w/o). Furthermore, an ambivalent range may be also emerged, where by the dispersed phase becomes the continuous one and vice versa. During this process the apparent viscosity of the mixture becomes very large, which leads to high pressure drops or low flow rates in pipeline transportation (see a review by Yeo et al.^[1]). In recent years, because of the presence of water in oil well or injection of water into the well for increasing oil production, oil extraction is often accompanied by a water throughput. Therefore, rheological research of oil and water emulsions is an important task in the field of rheology to find out ways for oil field development and petroleum transportation. So far, a vast amount of research has been done on the structure and properties

Received 21 August 2012; accepted 26 August 2012.

The authors gratefully acknowledge that the work described here is financially supported by the National Natural Science Foundation of China (No. 10902114), the Special Development of National Key Scientific Instruments in China (2011YQ120048-02), and the Outstanding Young Talent Incubation Program at Institute of Mechanics, Chinese Academy of Sciences.

Address correspondence to Jing-yu Xu, Institute of Mechanics, Chinese Academy of Sciences, Beijing 100190, P. R. China. E-mail: xujingyu@imech.ac.cn

of emulsions from different viewpoints for water-in-oil emulsions^[2-9] and for oil-in-water emulsions.^[10-16]

In the study of emulsions, handling and controlling the flow properties of emulsions is of a key interest for practical applications since it leads to a system with different physical behaviors. Generally, the flow properties are governed by different interaction forces that occur in the system, which in turn depend on volume fraction of the disperse phase, chemical composition of the continuous phase, interfacial properties, and concentration and nature of the emulsify agent. Other structural parameters important to the rheological characteristics of emulsions are properties of the continuous phase and droplet size and polydispersity.^[17] However, their impact on multiphase transportation has not yet been thoroughly investigated. The existing methods for determination and calculation of their rheological properties have not been optimized for use in multiphase simulations, such as the apparent viscosity of oil-water dispersed flow in pipeline.^[2,4,18] Most of results published in literature are based on steady oil and water dispersed system with emulsifying agent. In fact, from a practical point of view, the dispersed flow of oil and water two-phase usually are unsteady and coarse in the pipeline transportation. Only the system can be a fine stable structure if the water droplets are covered with surfactant or emulsifying agent.^[5] Nevertheless, much research is still urgently required in order to fully understand the flow properties of emulsions without emulsifying agent and the mechanisms behind it.

To improve the pipeline transportation of oil and water two-phase without emulsifying agent, we start this work as the following points. First, our subject for investigation is unsteady (coarse) emulsions, for which there are very limited publications devoted to this type emulsions. Second, it is considered necessary to carry out a full set of rheological measurements through the entire oil volume fractions, including the effects of system temperature, emulsifying agent and stirring time on the emulsions, in order to obtain the complete rheological characteristics of this type emulsion. Third, it seems to be very interesting to make systematic measurements on the emulsions during the phase inversion region to determine the effect of rheological characteristics on the phase inversion point.

2. EXPERIMENTAL

2.1. Materials

In this study, industry white oil PS-100 used for the preparation of emulsions is a refined mineral oil that consists of the saturated hydrocarbons, which were obtained from Yanshan Petrochemical Company in China and it is classified usually by the viscosity. At the temperature of 20°C, the white oil is characterized by a density of

840 kg/m³ and an oil-water interracial tension of 0.0315 N/m. Tap water is used as the water phase. The emulsions were prepared with fourteen different oil volume fractions (i.e., 5, 10, 20, 30, 40, 45, 50, 55, 60, 65, 70, 80, 90, 100 vol%). The homogenization was achieved by stirring the oil and water solutions with different time (90 seconds, 180 seconds, 300 seconds and 600 seconds) using the three-blade stirrer at a fixed speed (1000 r/m). After homogenization, the apparent viscosity and rheological characterization of oil-water emulsions were measured by exploiting the performance of the rheometer. The droplet sizes of samples were measured by taking photomicrographs of emulsions samples using a trinocular biological microscope model XSZ-H with an adapted digital camera (cannon 550D) operating at 100× magnification.

2.2. Emulsions Preparation

The samples were prepared in batches of 500 ml and pre-heated to a fixed test temperature. The steady (fine) emulsions were prepared by adding the emulsifying agent with 1.5 wt% and 600 seconds stirring. The commercial dodecylbenzene sulfonic acid sodium salt (SDBS) was used as the emulsifying agent supplied by Sinopharm Chemical Reagent Co., Ltd in China. The unsteady (coarse) emulsions without emulsifying agent were obtained by changing the stirring time from 90 to 600 seconds.

2.3. Rheological Measurements

Rheological measurements were carried out on a HAA-KERS6000 Rheometer with a coaxial cylinder sensor system (Z38 DIN, gap width = 2.5 mm and sample volume of 30.8 cm³) for the samples. A variety of temperature control units was also available to reliably and accurately handle temperatures ranging from -40 to 140°C. After positioning the sample on the sensor system, the corresponding measurement was started immediately to avoid the unsteady emulsions stratified. Most of the measurement tests were conducted under the CR mode and three replicates of each test were performed. If the repeatability of results measured is poor, CS mode would be used to repeat the measurement. Furthermore, this rheometer had a range of shear rate from 10⁻³ to 1500 s⁻¹ and a range of viscosity from 0.0005 Pas to 1000 Pas. In oscillatory measurements, an amplitude sweep at a fixed frequency of 1 Hz was performed prior to the following frequency sweep in order to ensure the selected stress was in the linear viscoelastic regions. Frequency ranged was from 0.1 to 100 rad/s.

3. RHEOLOGICAL ANALYSIS OF PURE OIL

The flow behavior of pure oil is investigated at six different temperatures over a wide range of shear rates from 1 to 200 s⁻¹. Figure 1a shows the variation of the sample viscosity with the shear rate. Overall, it is observed

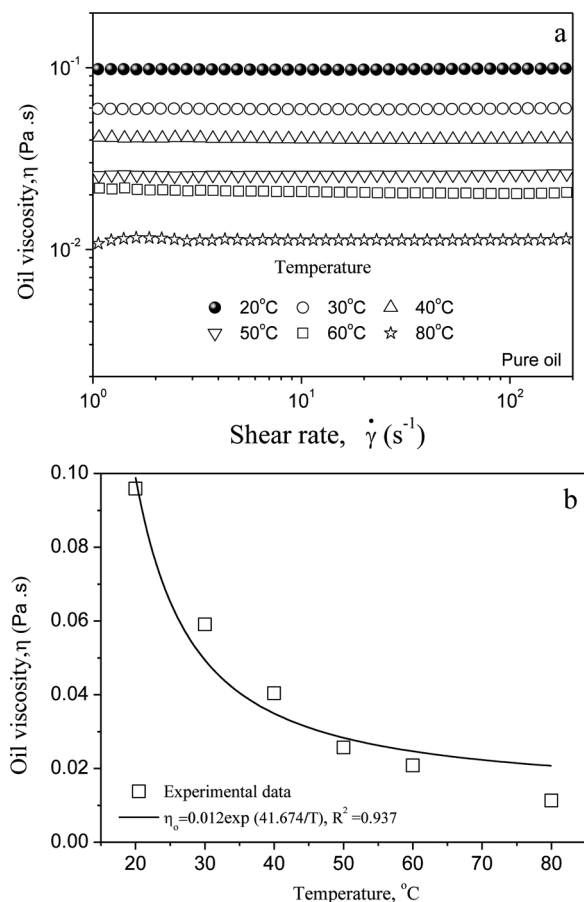


FIG. 1. Effect of temperature on the viscosity of pure oil under six different temperatures (a, shear rate vs. oil viscosity; b, temperature vs. oil viscosity).

that the viscosity of pure oil decreases with the increases of the temperature, and the sensitivity of the oil viscosity to temperature almost is not influenced by the shear rate when the shear rate remain at the measured range. All samples maintain the constant values with the increases of the shear rate and show Newtonian or quasi-Newtonian rheological behaviors.

It is well known that the oil viscosity (η_o) is a strong function of temperature. Usually, a plot of $\ln(\eta_o)$ versus $1/T$ yields a straight line with a positive slope. The relationship follows an Arrhenius-type equation as:

$$\eta_o = Ae^{B/T}, \quad [1]$$

here A and B are constants dependent on both system and shear rate. T is the absolute temperature in degree. Figure 1b gives a comparison of experimental data with the Arrhenius-type equation. The least squares method is used in identifying the appropriate exponential parameters. These results are given in Figure 1. It can be seen that

experimental data decrease exponentially with the system temperature. A good agreement between the data and fitting curves are obtained and the regression correlation coefficient (R^2) is 0.937.

4. APPARENT VISCOSITY OF OIL AND WATER EMULSIONS

According to the suggestions of Meriem-Benziane et al.^[8] and Hasan et al.,^[19] three rheological models of Ostwald de Waele model, Bingham model and Casson model are used to discuss the rheological behavior of oil-water emulsions in the present study, respectively.

The Ostwald de Waele model for emulsions is based on two parameters (m and n) in the following equation:

$$\tau = m(\dot{\gamma})^n, \quad [2]$$

here τ is the shear stress in Pa and $\dot{\gamma}$ is the corresponding shear rate in s^{-1} . The m and n are consistency index in $Pa s^n$ and flow behavior index.

The Bingham model for emulsions is described by two parameters (τ_o and η_a) in the following equation:

$$\tau = \tau_o + \eta_a(\dot{\gamma}), \quad [3]$$

here τ_o and η_a are the apparent yield stress in Pa and the apparent viscosity in Pa s, respectively.

The Casson model, similar to the Bingham model, can be also described by two parameters (τ_o and η_a) the following equation:

$$\tau = (\tau_o^{0.5} + (\eta_a \dot{\gamma})^{0.5})^2. \quad [4]$$

Equations (3) and (4) reflect the apparent yield stress for oil-water emulsions.

4.1. Effect of the Oil Volume Fraction

Figure 2 presents the dependence of apparent viscosity on shear rate for the samples with different oil volume fractions without emulsifying agent at 20°C. Generally, in a log-log coordinate, the curve of apparent viscosity against the shear rate shows the existence of a transition among three regions according to the oil volume fractions. In the low oil volume fractions ($\varepsilon_o = 0.05 \sim 0.30$), it can be noticed that the apparent viscosity of emulsion slightly increases with the shear rate increasing. With further increasing oil fraction ($\varepsilon_o = 0.40 \sim 0.70$), the apparent viscosity appears a reduction with shear rate increasing. However, in the high oil volume fractions ($\varepsilon_o = 0.80 \sim 1.0$), the apparent viscosity remains a constant value regardless of the shear rate. These findings show that the samples have different rheological behaviors base on the different oil volume fractions.

In the following study, we used three models (Equations (2)–(4)) to analyze the experimental data. The least squares method is used in identifying the appropriate model parameters. The results of the modeling analysis are reported in Table 1. It can be found that all three models give a very good regression correlation coefficient ($R^2 > 0.99$) for the emulsions with high oil volume fractions from 0.6 to 1, and the Ostwald de Waele model also show a good regression correlation coefficient ($R^2 > 0.98$) for the emulsions with low oil volume fractions from 0.05 to 0.3. However, for the emulsions with medium oil volume fractions from 0.4 to 0.55, the predictions of these models are far from satisfactory. Compared with other two models, The Casson model shows a relatively high regression correlation coefficient ($R^2 > 0.84$). The reason is due to the fact that the shear stress, for the emulsions with medium oil volume fractions, is reduced as the shear rate increasing at a high shear rate range ($600 \text{ s}^{-1} < \dot{\gamma}$). Furthermore, it can be also seen that with the increases of oil volume fraction, the flow behavior index (n) first decreases and then increases and but the apparent yield stress (τ_o) has an opposite tendency. These findings show that in the medium oil volume fractions, the emulsions have a stronger non-Newtonian fluid behavior that is the shear-thinning behavior as shown in the Figure 2.

Figure 3 depicts the apparent viscosity of emulsions against the oil volume fraction at three fixed shear rates. At low oil volume fractions, the apparent viscosity is small and increases sharply with the oil volume fraction increasing ($\varepsilon_o = 0.05 \sim 0.40$). When ε_o further increasing, the apparent viscosity tends to increase slowly and thereafter passes through a maximum and then decreases, and eventually

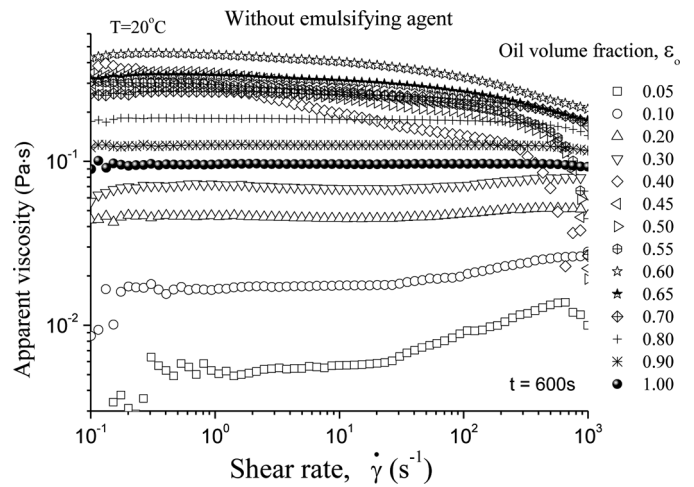


FIG. 2. Rheograms of the samples with different oil volume fractions without emulsifying agent at 20°C.

reaches to the single phase oil value. Over the range of $\varepsilon_o = 0.40 \sim 0.60$ the emulsions is unstable, which means that oil continuous regions (o/w) and water continuous regions (w/o) coexist (ambivalent range). Based on the experimental data, the apparent viscosity has a maximum around an oil volume fraction of 0.6 regardless of the changes of the shear rates. This is similar to previous findings (Miñana-Pérez et al.^[20]). They observed the maximum value was also about 0.6 using the stable emulsions. At this point the interaction between oil-continuous regions and water-continuous regions is the strongest. In the present study, this point is defined as the phase inversion point.^[2]

TABLE 1
Modeling evolution for emulsions without emulsifying agent at 20°C

Emulsions ε_o	Ostwald de Waele (Power) model			Bingham model			Casson model		
	m	n	R^2	τ_o	η_a	R^2	τ_o	η_a	R^2
0.05	0.0133	0.9811	0.9815	—	—	—	—	—	—
0.10	0.0118	1.1221	0.9996	—	—	—	—	—	—
0.20	0.0582	0.9769	0.9979	—	—	—	—	—	—
0.30	0.066	0.9472	0.9902	0.0354	0.0469	0.9892	—	—	—
0.40	1.7832	0.4459	0.8352	3.8132	0.0425	0.6197	0.4668	0.0482	0.8384
0.45	2.5133	0.4873	0.8030	5.7308	0.0803	0.6244	0.4900	0.0912	0.8491
0.50	2.1157	0.5117	0.8210	5.0160	0.0806	0.6645	0.3659	0.0808	0.8650
0.55	2.2623	0.5170	0.8442	5.4153	0.0898	0.6915	0.3829	0.1019	0.8798
0.60	0.7700	0.8110	0.9998	3.4663	0.2211	0.9888	0.1733	0.2249	0.9919
0.65	0.5964	0.8242	0.9997	2.5818	0.1872	0.9900	0.1001	0.1914	0.9934
0.70	0.5516	0.8323	0.9982	2.1097	0.1830	0.9884	0.0453	0.1892	0.9949
0.80	0.3033	0.8981	0.9988	0.9201	0.1552	0.9954	0.0080	0.1588	0.9983
0.90	0.1604	0.9554	0.9998	0.2747	0.1196	0.9992	0.0007	0.1209	0.9997
1	0.1124	0.9730	0.9999	0.1199	0.0941	0.9997	0.0001	0.0948	0.9999

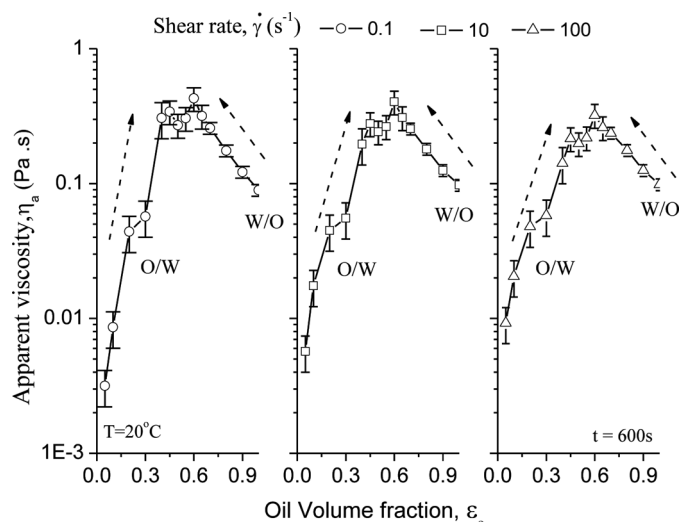


FIG. 3. Apparent viscosity as a function of oil volume fraction for different shear rates at 20°C.

4.2. Effect of Emulsifying Agent

An emulsifying agent has two important functions for oil-water emulsions, namely: a) to reduce the interfacial tension between oil and water and thereby enabling easier formation of the emulsions, and b) to stabilize the dispersed phase against coalescence once it is formed.^[21] Figure 4 shows that the effects of emulsifying agent on the apparent viscosity behavior for four different oil volume fractions ($\epsilon_o = 0.05, 0.40, 0.60,$ and 0.80). As be seen the emulsions of $\epsilon_o = 0.05$ without emulsifying agent has a different flow behavior, which is represented by a slightly viscoelastic shear-thickening. However, the adjunction of emulsifying agent makes this sample with a

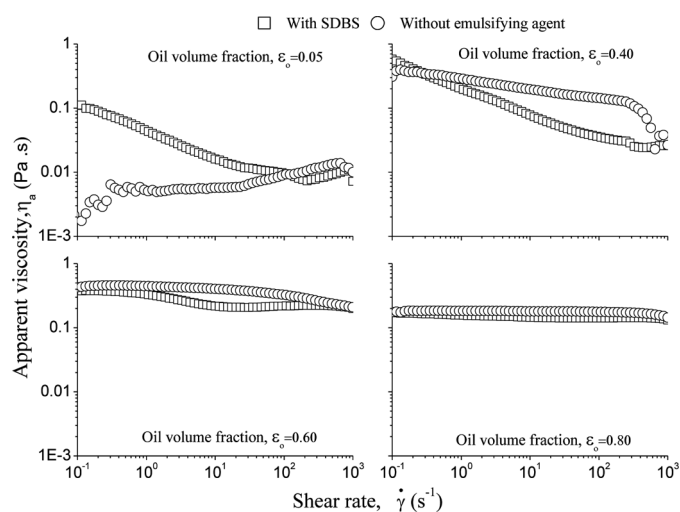


FIG. 4. Effect of emulsifying agent on the behavior of apparent viscosity for different oil volume fractions.

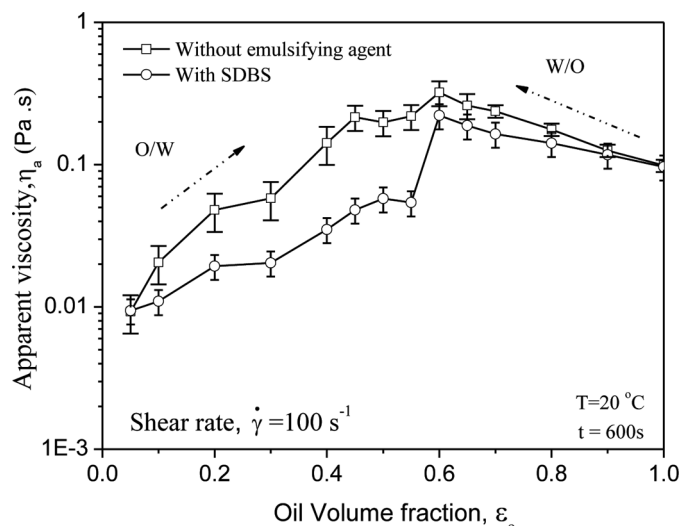


FIG. 5. Apparent viscosity as a function of oil volume fraction with or without emulsifying agent at a shear rate of 100 s^{-1} at 20°C.

transition from shear-thickening into shear-thinning, and enhances the apparent viscosity at a fixed low shear rate. With the increase of the oil volume fractions ($\epsilon_o = 0.40, 0.60,$ and 0.80), the apparent viscosity of samples with emulsifying agent become slightly lower than those without emulsifying agent, and show a similar shear-thinning behavior. Figure 5 gives the apparent viscosity against the oil volume fractions of the samples with or without emulsifying agent at a fixed shear rate ($\dot{\gamma} = 100\text{ s}^{-1}$). In general, the emulsifying agent reduces the apparent viscosity of samples and shows few influences on the trend of the curve and phase inversion point. The highest value of the apparent viscosity still appears at the oil volume fraction of 0.6.

4.3. Evaluation of the Apparent Viscosity Models

The apparent viscosity of emulsions is affected by a number of factors: viscosity of dispersed phase, density of dispersed phase, volume fraction of dispersed phase, viscosity of continuous phase, density of continuous phase, shear rate, system temperature, droplet size distribution, nature and concentration of emulsifying agents, and presence of solids in addition to dispersed phase and so on.^[4] In the last century, some models (empirical or semi-empirical) have been developed for predicting the apparent viscosity of oil-water emulsions. The models can generally be grouped into three main categories, namely, linear, exponential and power function models. Models used in the current study are presented in Table 2. In Table 2, η_r is the relatively viscosity, which is defined as the ratio of apparent viscosity of emulsions (η_a) to continuous phase viscosity (η_c). K is the ratio of dispersed phase viscosity to the continuous phase viscosity. \square and ϕ_m are the dispersed phase volume fraction and the maximum

TABLE 2
Models and correlations for the apparent viscosity of liquid-liquid dispersions in the literature

Authors, Year	Ref. no	Models and correlations	Category	Equation no.	Remarks
Einstein, 1906	[22]	$\eta_r = 1 + 2.5\phi$	Linear	(5)	Monodispersed system
Taylor, 1932	[23]	$\eta_r = 1 + \left(\frac{5K+2}{2K+2}\right)\phi$	Linear	(6)	Monodispersed system
Richardson, 1933	[24]	$\eta_r = \exp(C\phi)$	Exponential	(7)	C is constant by the experimental data regression
Guth and Simha, 1936	[25]	$\eta_r = 1 + 2.5\phi + 14.1\phi^2$	Power	(8)	Extension of Equation (5) to involve the interactions of droplet-droplet
Eilers, 1941	[26]	$\eta_r = \left(1 + \frac{1.25\phi}{1-k\phi}\right)^2$	Power	(9)	Extension of Equation (5) to polydispersed bitumen emulsions, $1.28 < k < 1.30$
Mooney, 1951	[27]	$\eta_r = \exp\left(\frac{2.5\phi}{1-k\phi}\right)$	Exponential	(10)	Extension of Equation (7) to predict the non-Newtonian behaviour, $1.35 < k < 1.91$
Roscoe and Brinkman, 1952	[28,29]	$\eta_r = (1 - \phi)^{-2.5}$	Power	(11)	Extension of Equation (5) to fit a high concentration emulsion
Yaron and Gal-Or, 1972	[30]	$\eta_r = 1 + \phi \left\{ \frac{5.5(4\phi^{7/3} + 10 - (84/11)\phi^{2/3} + (4/K)(1 - \phi^{7/3}))}{10(1 - \phi^{10/3}) - 25\phi(1 - \phi^{4/3}) + (10/K)(1 - \phi)(1 - \phi^{7/3})} \right\}$	Linear	(12)	Cell model by considering the hydrodynamic interaction between the neighboring droplets
Krigger and Dougherty, 1959	[31]	$\eta_r = \left(1 - \frac{\phi}{\phi_m}\right)^{-2.5\phi_m}$	Power	(13)	Correlation for concentrated solid spheres dispersions
Barnea and Mizrahi, 1975	[32]	$\eta_r = C \left(\frac{2(\beta C + K)}{C + K} \right), C = \exp \left[\frac{5\phi}{3(1-\phi)} \left(\frac{0.4+K}{1+K} \right) \right]$	Exponential	(14)	Developed for solid particles and extended to spherical liquid droplets.
Choi and Schowalter, 1975	[33]	$\eta_r = 1 + \phi \left\{ \frac{2[(5K+2) - 5(K-1)\phi^{7/3}]}{4(K+1) - 5(5K+2)\phi + 42K\phi^{5/3} - 5(5K-2)\phi^{7/3} + 4(K-1)\phi^{10/3}} \right\}$	Linear	(15)	Cell model by considering the hydrodynamic interaction between the neighboring droplets.
Barnea and Mizrahi, 1976	[34]	$\eta_r = 1 + C_1\phi + C_2\phi^2 + C_3\phi^3$	Power	(16)	Experimental data analysis required to fit the empirical constants ($C_1 \sim C_4$).
Pal and Rhodes, 1989	[21]	$\eta_r = [1 - (0.8415/\phi(100))\phi]^{-2.5}$	Power	(17)	Semi-empirical correlation by considering the effect of shear rate and is the dispersed phase concentration at relative viscosity is equal to 100.
Rønningsen, 1995	[35]	$\eta_r = \exp(C_1 + C_2T + C_3\phi + C_4T\phi)$	Exponential	(18)	Experimental data analysis required to fit the shear rate dependent coefficients ($C_1 \sim C_4$). T is system

(Continued)

TABLE 2
Continued

Authors, Year	Ref. no	Models and correlations	Category	Equation no.	Remarks
Phan-Thien and Pham, 1997	[36]	$\eta_r \left[\frac{2\eta_r + 5K}{2 + 5K} \right]^{1.5} = (1 - \phi)^{-2.5}$	Power	(19)	temperature. Extension of Equation (5) to fit the low concentration emulsions
Bicerano et al., 1999	[37]	$\eta_r = \left(1 - \frac{\phi}{\phi_m} \right)^{-2} \left[1 - 0.4 \left(\frac{\phi}{\phi_m} \right) + 0.34 \left(\frac{\phi}{\phi_m} \right)^2 \right]$	Power	(20)	Hard spherical droplets for dilute, semidilute and concentrated regimes.
Pal, 2000	[38]	$\eta_r \left[\frac{2\eta_r + 5K}{2 + 5K} \right]^{1.5} = \left(1 - \frac{\phi}{\phi_m} \right)^{-2.5}$	Power	(21)	Extension of Equation (19) including the maximum packing concentration volume fraction for uniform spheres
Pal, 2001	[39]	$\eta_r \left[\frac{2\eta_r + 5K}{2 + 5K} \right]^{1.5} = \exp \left(\frac{2.5\phi}{1 - \phi/\phi_m} \right)$ $\eta_r \left[\frac{2\eta_r + 5K}{2 + 5K} \right]^{1.5} = \left(1 - \frac{\phi}{\phi_m} \right)^{-2.5\phi_m}$	Exponential Power	(22) (23)	Extension of Equation (6) to concentrated emulsions of non-colloidal spherical droplets. $K \rightarrow \infty$, the Equation (22) reduce to Mooney (1951) and Equation (23) to Kringer and Dougherty (1959)

packing concentration volume fraction, respectively. All models are evaluated by using the experimental data except for Equations (7), (16), and (18). These are excluded because they require a lot of the experimental data analysis to fit the empirical constants.

Figure 6 shows the comparison of the apparent viscosity model against the experimental data without emulsifying agent at 20°C by using three different categories. It can be observed in Figure 6a that in the region of w/o, Equations (5), (12), and (15) give a good prediction. However, in the region of o/w, all the linear models under-predict the relative viscosity. Figure 6b presents the results by three exponential models. The exponential models have a good improvement over the medium range of oil volume fractions from 0.5 to 0.6. Equation (10) by Mooney^[27] seems close to the actual data of o/w for this range. The results predicted by the power models are demonstrated in Figures 6c and 6d. The results are similar to those by the exponential models. Compared with the results in the region of o/w, the models for the region of w/o show a better prediction results.

Overall, the linear model can better predict the relative viscosity in the region of w/o besides of Equation (6). During the medium region ($\varepsilon_o = 0.50 \sim 0.60$), the exponential model of Equation (10) and the power models of Equations (20) and (21) are closer to the actual data of the emulsions without emulsifying agent. A comparison of the predicted curves with the experimental data shows that, for the high oil volume fractions ($\varepsilon_o > 0.50$), the Equation (21) by Pal^[38] is suitable to predict the relative viscosity.

However, it can be also concluded that all theoretical model under-predict the relative viscosity for the emulsions of o/w with low oil volume fractions ($\varepsilon_o = 0.05 \sim 0.50$). The main reason for this deviation is believed to be the fact that most of the models for predicting the relative viscosity with low volume fraction are developed base on steady and fine emulsions. In this study, the emulsions without emulsifying agent are coarse and unsteady, especially for the emulsions with low oil volume fraction. Figure 7 shows the photos of natural phase separation after stirring 600 seconds. It can be found that there are natural layers of oil and water after 5 minutes stirring due to the droplet-droplet fast hydrodynamic interactions (flocculation) and the density difference between oil and water.

5. RHEOLOGICAL CHARACTERISTICS OF THE EMULSIONS AT THE PHASE INVERSION POINT

In the present study, the maximum value of the apparent viscosity is around an oil volume fraction of 0.6 regardless of the changes of the shear rate and the emulsifying agents, as shown in Figures 3 and 5. Thus, in the following experiments, we investigate on rheological characteristics of the emulsions at this point. Knowledge of the droplet size of

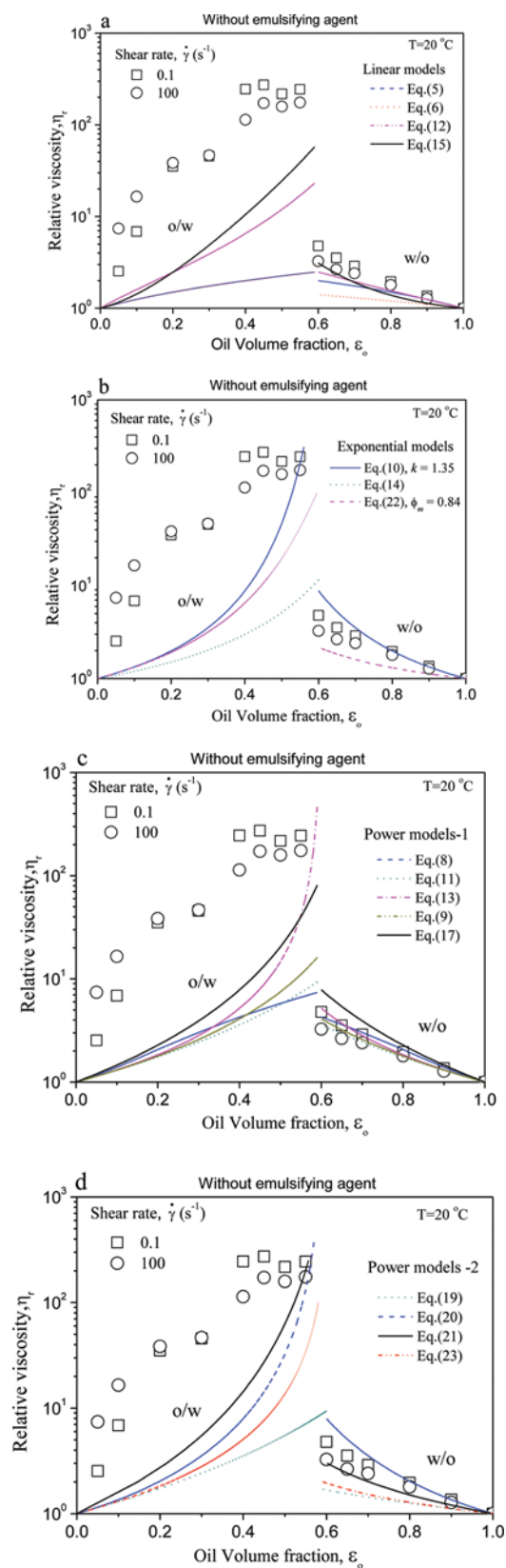


FIG. 6. Comparison of the apparent viscosity models against experimental data at 20°C. (Figure available in color online.)

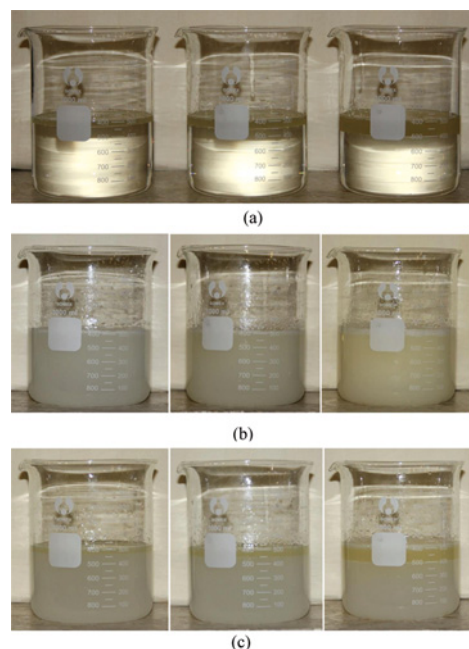


FIG. 7. Natural phase separation for the unsteady of (coarse) emulsions at the low oil fractions without emulsifying agent. a) Original sample with different oil volume fractions prior to the stirring (from left to right: $\epsilon_o = 0.05, 0.10$ and 0.20). b) Emulsions with different oil volume fractions after 600 seconds stirring (from left to right: $\epsilon_o = 0.05, 0.10$ and 0.20). c) Settlement after 5 minutes (from left to right: $\epsilon_o = 0.05, 0.10$ and 0.20). (Figure available in color online.)

the dispersed phase and its polydispersity is important in characterizing emulsion stability and improving the understanding of the emulsification process.^[40] The droplets size and polydispersity of the dispersed phase are determined by two opposing mechanisms, droplet breakup and coalescence, that occur simultaneously when the emulsions are exposed to shear. Therefore, under the conditions of the shear with an enough long time, a dynamic equilibrium will be established between breakup and coalescence, resulting in an apparent equilibrium in droplet size and size distribution.^[2] In the following work, to study the effects of droplet size and distribution on the emulsions, four different stirring time are carried out on the emulsions at an identical oil volume fraction ($\epsilon_o = 0.60$).

5.1. Effect of Stirring Time on the Stability

Figure 8 shows the effects of stirring time on the steady of emulsions without emulsifying agent. As be shown, the droplet sizes of the emulsions for 600 seconds stirring are much smaller than those of the 90 seconds stirring. The emulsions with a short time stirring is very unsteady and fast stratified after 5 min. The steady can be enhanced with the stirring time increased. Figure 9 gives the micrography ($100\times$) for the effect of stirring time on emulsions corresponding to Figure 8b. Clearly, the longer the stirring

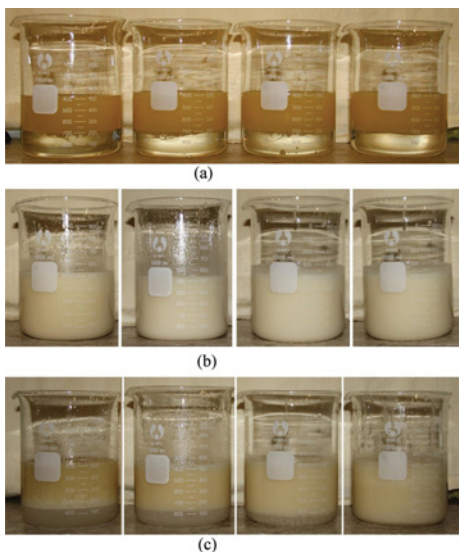


FIG. 8. Effect of stirring time on the steady of emulsions at the phase inversion point without emulsifying agent. a) Original sample prior to the stirring with 0.60 oil volume fraction. b) Emulsions with different stirring time (from left to right: 90 seconds, 180 seconds, 300 seconds and 600 seconds). c) Settlement after 5 minutes (from left to right: 90 seconds, 180 seconds, 300 seconds and 600 seconds). (Figure available in color online.)

time is, the smaller the droplet size. Also, the coarse emulsion (90 seconds stirring) appears to have a width distribution of droplet sizes and also exhibits a greater tendency to flocculate. The approximate values of volume average droplet sizes of emulsions are 60 μm , 35, 18, and 6 μm for the stirring time 90, 180, 300, and 600 seconds, respectively. The droplet size distributions for 90 seconds stirring on the emulsions of 0.6 oil volume fraction is described in Figure 10.

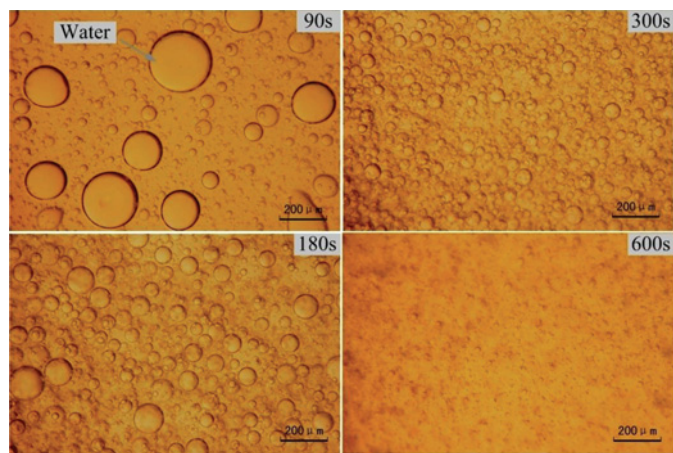


FIG. 9. Micrography (100 \times) for the effects of stirring time on water-in-oil emulsions at oil volume fraction, $\epsilon_o = 0.60$. (Figure available in color online.)

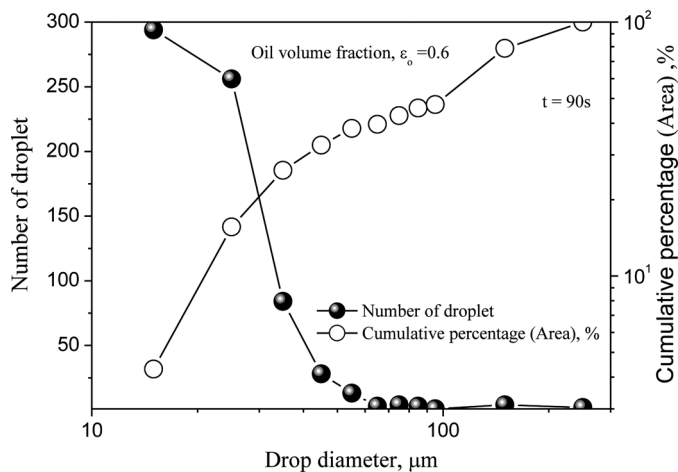


FIG. 10. Droplet size distributions for the emulsions with 0.60 oil volume fraction at 90 seconds stirring.

Figure 11 presents that the rheograms of the emulsions for four different stirring time. It can be observed that at a fixed shear rate the shear stress increases with the stirring time lengthened. The simulation of yield stress of the emulsions with different stirring time by the Bingham and Casson models are also shown in Table 3, respectively. Validations of these models are done on the basis of the coefficient R^2 that are closed to unity. Thus, the values of the yield stress show a good prediction by the Bingham and Casson models ($R^2 > 0.99$). The yield point (τ_o) required to start the flow of emulsions increases with the stirring time lengthened. Predicted by the Bingham model, the yield point remains a value of 1.4012 Pa with 90 seconds and it increases to 3.4663 Pa when the stirring time

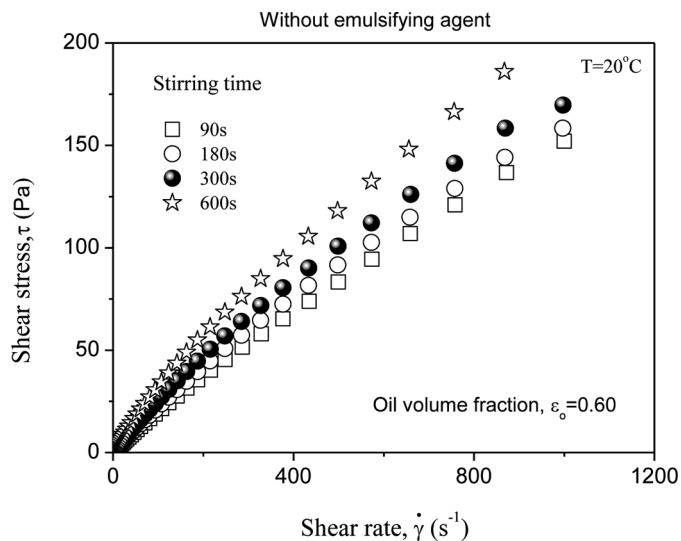


FIG. 11. Rheograms of the emulsions with 0.6 oil volume fraction for four different stirring time.

TABLE 3

Simulation values of flow behavior index and yield stress for the emulsions of 0.6 oil volume fraction with different stirring time at 20°C

Stirring time seconds	Bingham model		Casson model	
	τ_o (Pa)	R^2	τ_o (Pa)	R^2
90	1.4012	0.9958	0.0376	0.9973
180	1.8713	0.9920	0.0527	0.9958
300	2.4295	0.9891	0.0782	0.9940
600	3.4663	0.9888	0.1733	0.9919

lengthened to 600 seconds. It means that this emulsions with a long stirring time (small droplet sizes) requires a relatively high energy to start flowing and suffers many transportation problems, such as a shutdown and a restart of the pumping the pipeline.^[16]

Figure 12 depicts the apparent viscosity at a function of shear rate under different stirring time. The emulsions show a strong shear-thinning behavior, especially for the emulsion with 600 seconds stirring. Combining Figure 9 with Figure 12, it can be concluded that the emulsions with a size distribution dominated by small droplets have a higher viscosity than those with a higher average droplet size a tan identical oil volume fraction ($\epsilon_o = 0.60$ in this work). It has also been obtained that the apparent viscosity becomes higher when the degree of polydispersity in the system is low, that is, the size distribution is narrow.

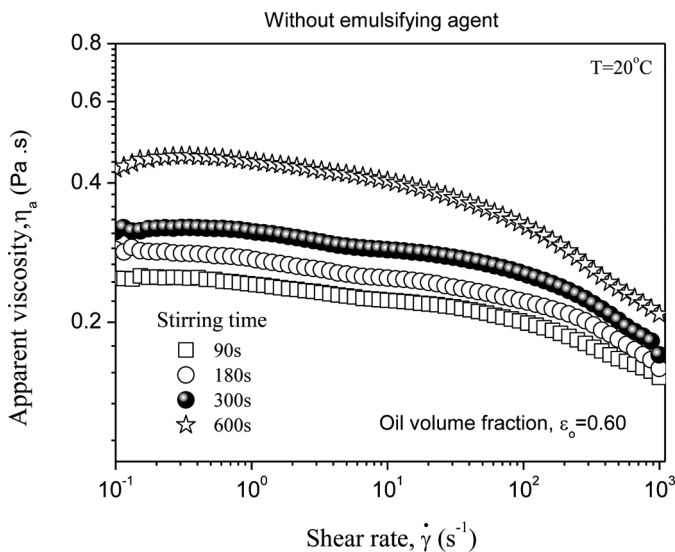


FIG. 12. Apparent viscosity at a function of shear rate with 0.6 oil volume fraction under different stirring time.

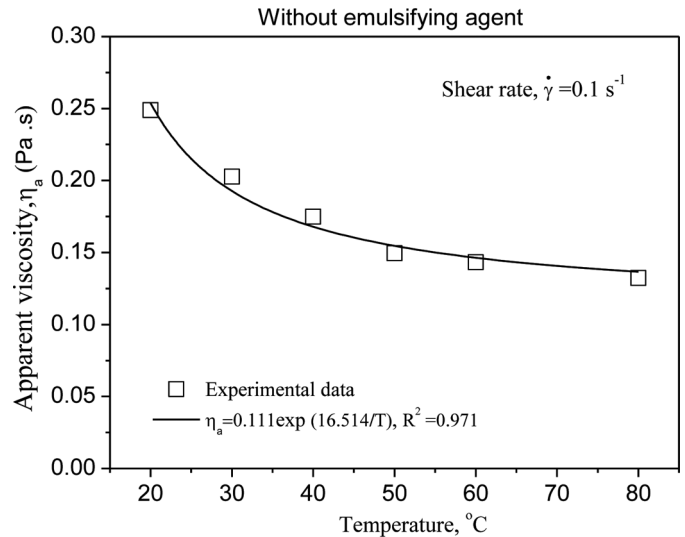


FIG. 13. Apparent viscosity at a function of system temperature for emulsion at 60% oil volume fraction.

5.2. Effect of System Temperature

It is well-known that the system temperature has an important effect on the apparent viscosity of emulsions. For instance, a reduction of temperature causes a remarkable increase in the viscosity of continuous phase. Figure 13 shows that the effects of system temperature on the apparent viscosity behavior at the phase inversion point. It can be seen that experimental data decrease exponentially with the system temperature. The tendency of curve is similar to the pure oil (Figure 1b). The relationship of Arrhenius-type (Equation (1)) is also used to analysis the data. A good agreement between the data and fitting curves are obtained and the regression correlation coefficient (R^2) is 0.971.

5.3. Viscoelastic Property of the Emulsions

Figure 14 gives the variations of the complex viscosity, the elastic modulus, and the loss modulus with the shear stress at a fixed frequency for the emulsions of four different stirring time with or without emulsifying agent. Measurements are undertaken to obtain these parameters for recognizing the linear viscosity region. An important point to note is that in the case of the emulsions without emulsifying agent (Figure 14a), the loss modulus is greater than the storage modulus over the entire shear stress range, indicating these emulsions are predominantly viscosity. Furthermore, with shear stress increases, the complex viscosity and the loss modulus slightly decreases and but the elastic modulus is slightly increased. There appears to be two weak linear intervals: (a) $0.1 \text{ Pa} < \tau < 5 \text{ Pa}$ and (b) $5 \text{ Pa} < \tau < 100 \text{ Pa}$. With the stirring time lengthened the linear feature is enhanced. However, for the emulsion with SDBS, the Figure 14b demonstrates that at a fixed

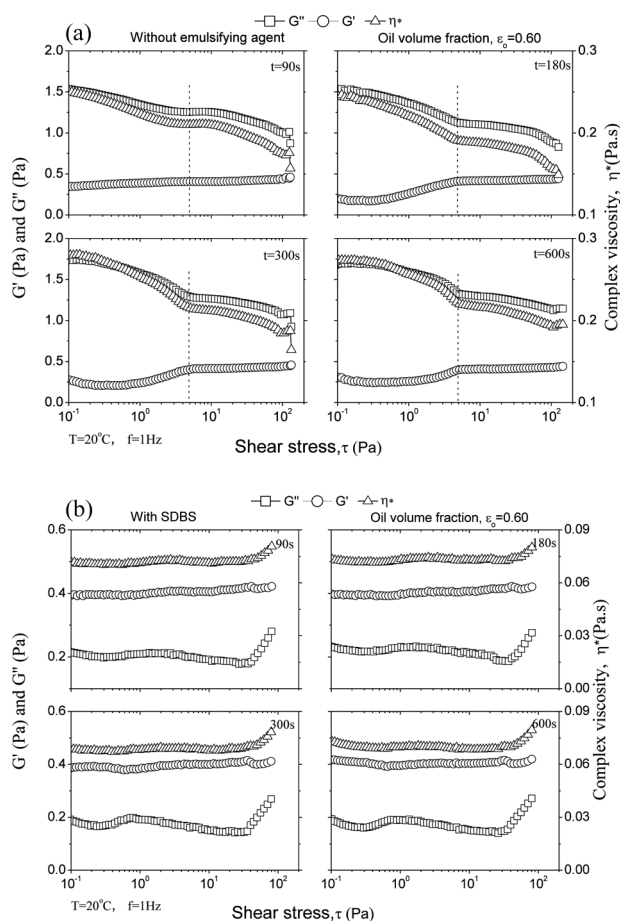


FIG. 14. Variations of the complex viscosity, the elastic modulus, and the loss modulus with the shear stress at a fixed frequency for different stirring time with SDBS at 0.60 oil volume fraction (a, emulsions without emulsifying agent; b, emulsions with SDBS).

frequency ($f=1$ Hz), the shear stress dependence of the complex viscosity, the elastic modulus, and the loss modulus is rather weak. The linearity of viscoelastic behavior of emulsions is good and continues to be in a rather wide range of stress amplitudes (from 0.1 Pa to 50 Pa). Moreover, the loss modulus is much lower than storage modulus. This result corresponds to a predominantly elastic behavior of the emulsion with SDBS during the phase inversion point at a fixed frequency.

Figure 15 describes the ratio of the elastic modulus to the loss modulus (G'/G'') and the phase angles as a function of the shear stress at a fixed frequency. It can be observed that the G'/G'' slightly depends on the shear stress. Here the ratio of the elastic modulus to the loss modulus reflects two regimes: Viscous (if $G'/G'' < 1$) and Elastic (if $G'/G'' > 1$). Values for the phase angles gives information about the nature of the viscoelastic response of the emulsions system. In elastic networks, the phase angle shift is 0° while in purely viscous liquids it is 90° . For viscoelastic systems, the phase angle shift ranges

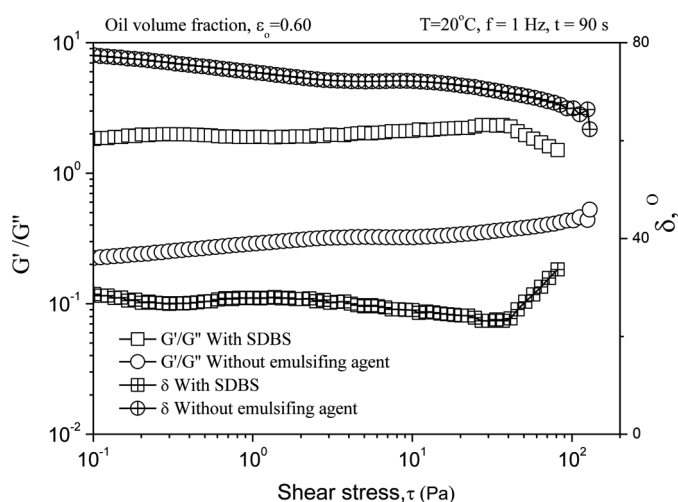


FIG. 15. Ratio of the elastic modulus to the loss modulus (G'/G'') and the phase angles as a function of the shear stress at a fixed frequent.

between 0° and 90° . The closer the phase angle shift to 0° , the more the emulsions system displays an elastic response to the shear stress. It can be found in Figure 15 that the phase angle is between 20° and 40° for the emulsions with SDBS, and between 60° and 80° for the emulsions without emulsifying agent. Thus, more gel-like network is developed in the emulsions with SDBS than the emulsions without emulsifying agent.^[8,41]

For a fixed shear stress, Figure 16 gives the plots of the complex viscosity, the elastic modulus, and the loss modulus against the frequency for 90 seconds stirring time (coarse emulsions) with or without emulsifying agent. As shown in Figure 16a, the emulsions without emulsifying agent, a liquid-like behavior is observed at lower frequency ($G' < G''$;) and a solid-like behavior observed at higher frequency ($G' > G''$). The crossover frequency ($G' = G''$) is found to be around $\omega = 30$ rad/s and almost is not vary with the shear stress increased from 0.1 Pa to 100 Pa. Furthermore, the complex viscosity exhibits a plateau region in the low frequency from 0.5 rad/s to 30 rad/s and then sharply increases with frequency further increasing. Figure 16b shows the results of emulsions with SDBS. Compared Figures 16a and 16b, it can be found that the addition of SDBS in the emulsions leads to a reduction of the value at the crossover point. With the increases of shear stress, the value at crossover point becomes smaller for the emulsion with SDBS over the entire range of frequency. Furthermore, the complex viscosity of the emulsions with SDBS is lower than those without emulsifying agent.

Figure 17 gives that the ratio of the elastic modulus to the loss modulus (G'/G'') and the phase angles as a function of the frequency at a fixed shear stress ($\tau = 10$ Pa). A transition between the elastic and the viscous behavior can be obtained at $\delta = 60^\circ$. Over the entire frequency

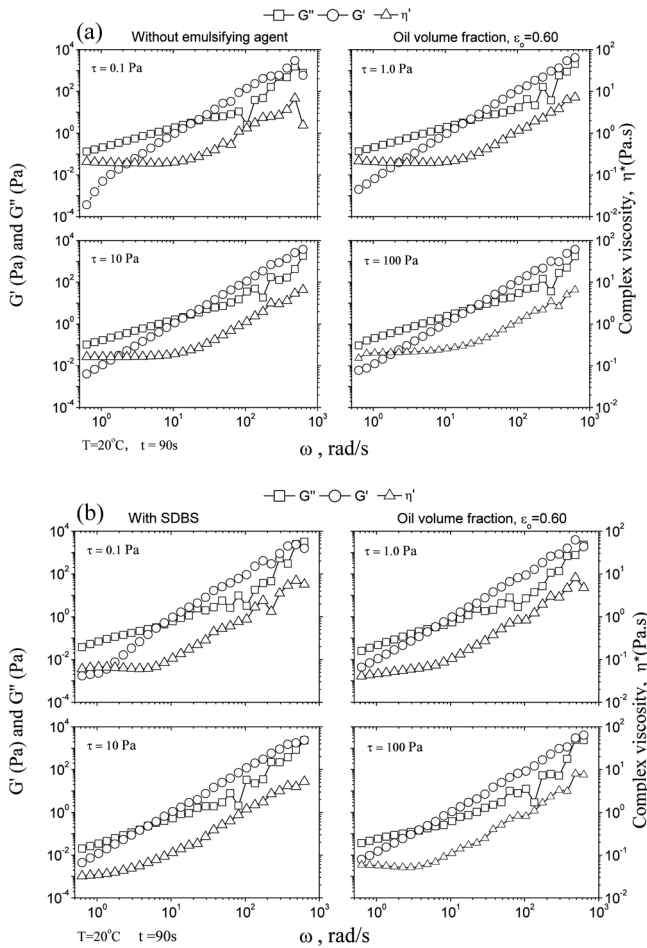


FIG. 16. Variations of the complex viscosity, the elastic modulus, and the loss modulus with the frequency at different shear stresses for 90 seconds stirring (a, emulsions without emulsifying agent; b, emulsions with SDBS).

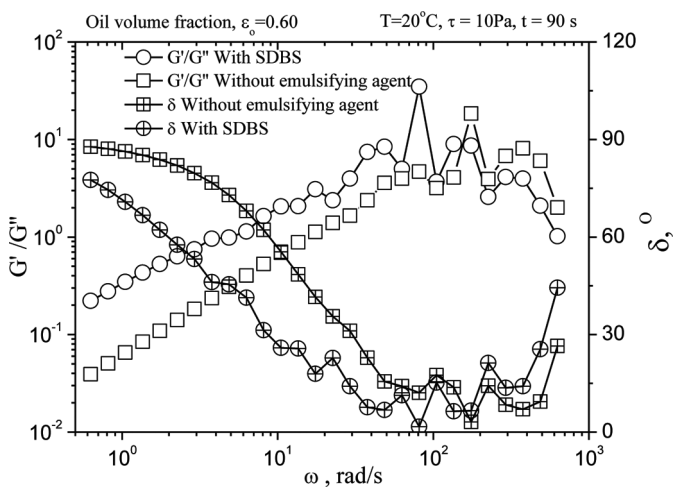


FIG. 17. Ratio of the elastic modulus to the loss modulus (G'/G'') and the phase angles as a function of the frequency at a fixed shear stress.

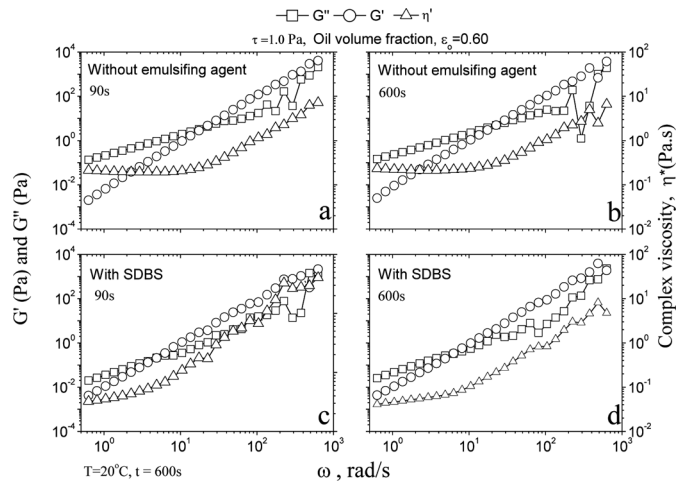


FIG. 18. Variations of the complex viscosity, the elastic modulus, and the loss modulus with the frequency at a fixed shear stresses for 90 and 600 seconds stirring, respectively. (a, 90 seconds stirring without emulsifying agent; b, 600 seconds stirring without emulsifying agent; c, 90 seconds stirring with SDBS; d, 600 seconds stirring with SDBS).

interval, the rheological behavior of the emulsion is changed from viscous fluid to elastic fluid with the frequency increasing. Emulsifying agent makes the emulsion possessing more elasticity. Based on the change of G'/G'' with frequency increasing, the emulsions appear a non-linear viscoelastic behavior and not follow the general Maxwell model.

Finally, the effects of stirring time on the rheological behavior at the phase version point have been investigated. The results are shown in Figure 18 with two different stirring time at a fixed shear stresses ($\tau = 1 \text{ Pa}$). It is noted that the stirring time has few influence on two modulus and complex viscosity. In the emulsions with SDBS, the plateau region of complex viscosity disappears and continuously increases with frequency increasing.

6. CONCLUDING REMARKS

To improve the pipeline transportation of oil and water two-phase, the emulsions of oil and water through the entire oil volume fractions is studied, including the effects of system temperature, emulsifying agent and stability on the emulsions. Based on the experimental results and analysis, the following conclusions can be obtained:

1. The rheological properties of emulsions studied are significantly influenced by their oil volume fraction, stirring time and emulsifying agent. The emulsifying agent is found to reduce the apparent viscosity, and the stirring time lengthened (i.e., reduction in droplet size) results in a dramatic increase in the viscosity. However, both emulsifying agent and shear rate have few influence on the phase inversion point and the maximum value of the apparent viscosity appears around $\epsilon_o = 0.60$.

2. The emulsions with different volume fractions are distinguished by three rheological models as followed: Ostwald de Waele model for emulsions with low oil fractions ($\varepsilon_o = 0.05 \sim 0.40$, region of o/w); Casson model for emulsions with medium oil fractions as an acceptable prediction ($\varepsilon_o = 0.40 \sim 0.55$, ambivalent range); Ostwald de Waele model, Bingham model and Casson model for emulsions with high oil fractions ($\varepsilon_o = 0.60 \sim 1.0$, region of w/o).
3. The apparent viscosity models published in the literature are divided in to three categories, namely linear, exponential and power models, and evaluated by using the experimental data in this work. In general, most of the models can give a good prediction for the emulsions with high oil fractions ($\varepsilon_o = 0.60 \sim 1.0$, region of w/o). However, the experimental data for the emulsions exhibit large deviations from the existing theoretical models over the range of low oil fractions $\varepsilon_o < 0.5$, region of o/w). The model of Pal,^[38] covering a relative broad range of oil volume fractions ($\varepsilon_o = 0.50 \sim 1.0$), are suitable to predict the relative viscosity.
4. At the phase inversion point ($\varepsilon_o = 0.60$), the behavior of the viscoelastic emulsions are analyzed by the shear stress sweeps and frequency sweeps of the emulsions, respectively. In general, for the shear stress sweeps, the addition of emulsifying agent results in the emulsions with a transition from a liquid-like behavior into a solid-like behavior. For the frequency sweeps, the emulsifying agent reduces the value at the crossover frequency and decreases the complex viscosity of the emulsions. Furthermore, the stirring time (i.e., droplet size and distribution) has few influences on the elastic modulus and the loss modulus.

REFERENCES

- [1] Yeo, L.Y., Matar, O.K., Perez de Ortiz, E.S., and Hewitt, G.F. (2000) *Multiphase Sci. Technol.*, 12: 51–116.
- [2] Urdahl, O., Fredheim, A.O., and Løken, K.P. (1997) *Colloid Surf. A*, 123–124: 623–634.
- [3] Jager-Lézer, N.J., Tranchant, J.-F., Alard, V., Vu, C., Tchoreloff, P.C., and Grossiord, J.-L. (1998) *Rheol. Acta*, 37: 129–138.
- [4] Johnsen, E.E. and Rønningsen, H.P. (2003) *J. Petr. Technol.*, 38: 23–36.
- [5] Masalova, I., Malkin, A.Y., Slatter, P., and Wilson, K. (2003) *J. Non-Newtonian Fluid Mech.*, 112: 101–114.
- [6] Malkin, A.Y., Massalova, I., Slatter, P., and Wilson, K. (2004) *Rheol. Acta*, 43: 584–591.
- [7] Rensing, P.J., Liberatore, M.W., Sum, A.K., Koh, C.A., and Sloan, E.D. (2011) *J. Non-Newtonian Fluid Mech.*, 166: 859–866.
- [8] Meriem-Benziane, M., Abdul-Wahab, S.A., Benaicha, M., and Belhadri, M. (2012) *Fuel*, 95: 97–107.
- [9] Maia Filho, D.C., Ramalho, J.B.V.S., Spinelli, L.S., and Lucas, E.F. (2012) *Colloid Surf. A*, 396: 208–212.
- [10] Otsubo, Y. and Prud'homme, R.K. (1994) *Rheol. Acta*, 33: 303–306.
- [11] Pal, R. (1995) *AIChE J.*, 41: 783–794.
- [12] Pal, R. (1996a) *Chem. Eng. Sci.*, 51: 3299–3305.
- [13] Ahmed, N.S., Nassar, A.M., Zaki, N.N., and Gharieb, H.K. (1999a) *Petr. Sci. Technol.*, 17: 553–576.
- [14] Ahmed, N.S., Nassar, A.M., Zaki, N.N., and Gharieb, H.K. (1999b) *Fuel*, 78: 593–600.
- [15] Elgibaly, A.A., Nashawi, I.S., Tantawy, M.A., and Elkamel, A. (1999) *J. Dispersion Sci. Technol.*, 20: 857–882.
- [16] Zaki, N., Butz, T., and Kessel, D. (2001) *Petr. Sci. Technol.*, 19: 425–435.
- [17] Partal, P., Guerrero, A., Berjano, M., and Gallegos, C.J. (1997) *Am. Oil Chem. Soc.*, 74: 1203–1212.
- [18] Xu, J.Y., Li, D.H., Guo, J., and Wu, Y.X. (2010) *Int. J. Multiphase Flow*, 36: 930–939.
- [19] Hasan, S.W., Ghannam, M.T., and Esmail, N. (2010) *Fuel*, 89: 1095–1100.
- [20] Miñana-Perez, M., Jarry, P., Pérez-Sánchez, M., Ramirez-Gouveia, M., and Salager, J.L. (1986) *J. Dispersion Sci. Technol.*, 7: 331–343.
- [21] Pal, R. and Rhodes, E. (1989) *J. Rheol.*, 33: 1021–1045.
- [22] Einstein, A. (1906) *Ann. Phys.*, 19: 289–306.
- [23] Taylor, G.I. (1932) *Proc. R. Soc.*, 138: 41–48.
- [24] Richardson, E.G. (1933) *Kolloid-Z.*, 65: 32–37.
- [25] Guth, E. and Simha, R. (1936) *Kolloid-Z.*, 74: 266–275.
- [26] Eilers von, H. (1941) *Kolloid-Z.*, 97: 313–321.
- [27] Mooney, M. (1951) *J. Colloid Sci.*, 6: 162–170.
- [28] Roscoe, R. (1952) *Br. J. Appl. Phys.*, 3: 267–269.
- [29] Brinkman, H.C. (1952) *J. Chem. Phys.*, 20: 571–581.
- [30] Yaron, I. and Gal-Or, B. (1972) *Rheol. Acta*, 11: 245–252.
- [31] Krieger, I.M. and Dougherty, T.J. (1959) *J. Rheol.*, 3: 137–152.
- [32] Barnea, E. and Mizrahi, J.A. (1975) *Can. J. Chem. Eng.*, 53: 461–468.
- [33] Choi, S.J. and Schowalter, W.R. (1975) *Phys. Fluids*, 18: 420–427.
- [34] Barnea, E. and Mizrahi, J. (1976) *Ind. Eng. Chem. Fundam.*, 15: 120–125.
- [35] Rønningsen, H.P. (1995) Proceedings of the SPE International Symposium on Oil Field Chemistry, Houston TX, P28968.
- [36] Phan-Thein, N. and Pham, D.C. (1997) *J. Non-Newtonian Fluid Mech.*, 72: 305–318.
- [37] Bicerano, J., Douglas, J.F., and Brunea, D.A. (1999) *Polym. Rev.*, 39: 561–642.
- [38] Pal, R. (2000) *J. Colloid Interf. Sci.*, 231: 168–175.
- [39] Pal, R. (2001) *J. Rheol.*, 45: 509–520.
- [40] Pal, R. (1996b) *AIChE J.*, 42: 3181–3190.
- [41] Hejazi, I., Seyfi, J., Sadeghi, G.M.M., and Davachi, S.M. (2011) *Mater. Design*, 326: 49–55.